Cardiovascular Drugs and Therapy (2020) 34:475–485
https://doi.org/10.1007/s10557-020-06986-y

ORIGINAL ARTICLE

# Single-Strand DNA-Like Oligonucleotide Aptamer Against Proprotein Convertase Subtilisin/Kexin 9 Using CE-SELEX: PCSK9 Targeting Selection

Roohollah Sattari[1] · Abbasali Palizban[1] · Hossein Khanahmad[2]

Published online: 15 May 2020


## Abstract

**Background** Proprotein convertase subtilisin/kexin 9 (PCSK9) serves a key regulatory function in the metabolism of low-density lipoprotein (LDL)-cholesterol (LDL-C) through interaction with the LDL receptor (LDLR) followed by its destruction that results in the elevation of the plasma levels of LDL-C. The aims of the present study were to separate and select a number of single-stranded DNA (ssDNA) aptamers against PCSK9 from a library pool ($n > 10^{12}$) followed by their characterization.

**Methods** The aptamers obtained from the DNA-PCSK9 complexes which presented the highest affinity against PCSK9 were separated and selected using capillary electrophoresis evolution of ligands by exponential enrichment (CE-SELEX). The selected aptamers were amplified and cloned into a T/A vector. The plasmids from the positive clones were extracted and sequenced. The Mfold web server was used to predict the secondary structure of the aptamers.

**Results** Following three rounds of CE-SELEX, the identified anti-PCSK9 ssDNA aptamers, namely aptamer 1 (AP-1) and aptamer 2 (AP-2), presented half maximal inhibitory concentrations of 325 and 327 nM, lowest dissociation constants of 294 and 323 nM, and most negative Gibbs free energy values of − 9.17 and − 8.28 kcal/mol, respectively.

**Conclusion** The results indicated that the selected aptamers (AP-1 and AP-2) induced potent inhibitory effects against PCSK9. Further in vivo studies demand to find out AP-1 and AP-2 aptamers as suitable candidates, instead of antibodies, for using in therapeutic purposes in patients with hypercholesterolemia and cardiovascular disease.

**Keywords** Single-stranded DNA aptamer · Proprotein convertase subtilisin/kexin type 9 · Capillary electrophoresis evolution of ligands by exponential enrichment · Cardiovascular disease

## Introduction

Despite numerous studies with rapid advances having been performed in the field of cardiovascular diseases (CVDs), they remain the leading cause of mortality globally [1]. Increased levels of atherogenic lipoproteins, including low-density lipoprotein-cholesterol (LDL-C), intermediate-density lipoprotein-cholesterol, very low-density lipoprotein-cholesterol, and lipoprotein (a) in the bloodstream are associated with an elevated risk of CVD [2]. It has been determined that ~ 70% of plasma cholesterol is carried in LDL, a well-known factor used for the evaluation of the risk of CVD. On the other hand, the LDL receptor (LDLR) serves a key role in the regulation of plasma cholesterol level [3]. The application of various strategies aiming to lower LDL-C has long been considered to be effective in preventing CVD and reducing the progression of atherosclerosis [4]. As demonstrated by numerous prospective clinical trials, LDL-C reduction is considered to be an effective intervention to reduce cardiovascular-associated morbidity and mortality rates [5]. Familial hypercholesterolemia (FH) is characterized by increased levels of LDL-C and a risk of premature CVDs due to the deficiency in the uptake of LDL-C by LDLR [6].

In 2003, the newest member of the proprotein convertase family, proprotein convertase subtilisin/kexin 9 (PCSK9), was introduced by Seidah et al [7]. In the same year, Abifadel et al

✉ Abbasali Palizban
palizban@pharm.mui.ac.ir

[1] Department of Clinical Biochemistry, Faculty of Pharmacy and Pharmaceutical Sciences, Isfahan University of Medical Sciences, Hezar Jerib Street, Isfahan 817467346, Iran

[2] Department of Molecular Biology and Genetics, Faculty of Medicine, Isfahan University of Medical Sciences, Isfahan 8174673461, Iran

[8] identified mutations which were not associated with the genetic variations of LDLR or apolipoprotein B. These mutations result in an increase in the gene expression level of PCSK9 which results in a novel clinical syndrome, termed FH3 that is not recognizable when compared with the conventional FH phenotype [8].

The PCSK9 gene is located on the short arm of chromosome 1 (1p32.3) and is primarily expressed in the liver, and to a lesser extent, in the intestine, kidney, pancreas, and central nervous system. PCSK9 is expressed as a zymogen (preproPCSK9) which consists of 692 amino acids and weighs 74 kDa. It is comprised of a signal peptide, pro-domain, catalytic domain, hinge region, and a cysteine/histidine-rich domain at the C-terminal. The conversion of preproPCSK9 to proPCSK9 in the endoplasmic reticulum occurs through the cleavage of a fragment of the peptide. The mature form of PCSK9 is then produced via autocatalytic action [9]. Mature PCSK9 serves a key function in the metabolism of LDL-C on the surface of hepatocytes, through interaction with the LDLR followed by its degradation, which results in an increase in the plasma level of LDL-C [10].

Recently, three mechanisms of controlling PCSK9 have been identified. The first mechanism prevents the binding of PCSK9 to the LDLR and comprises of monoclonal antibodies (mAbs), mimetic peptides, or adnectins, also termed monobodies [11]. The second mechanism includes the inhibition of the expression and synthesis of PCSK9. Examples of the second mechanism include clustered regularly interspaced short palindromic repeats/CRISPR-associated protein 9 technology, small molecules (berberine and oleanolic acid), antisense oligonucleotides, and small interfering RNAs [12]. The third mechanism comprises the interruption of PCSK9 secretion. For instance, two particular proteins, namely sortilin and SEC24 homolog A, COPII coat complex component, are known to be involved in PCSK9 secretion [13]. At present, the application of monoclonal antibodies has been proposed to be an effective approach of preventing the interaction between PCSK9 and LDLR [14]. By blocking the combination of PCSK9 and LDLR, the mAbs may lower LDL-C levels by 40–70% in patients with heterozygous FH and without FH [15].

Aptamers, the biomolecular ligands composed of single-stranded DNA (ssDNA) or RNA oligonucleotides, are developed by an in vitro selection process known as systematic evolution of ligands by exponential enrichment (SELEX) [16]. It has been indicated that aptamers may bind to a variety of molecules; therefore, they may be applied for diagnostic or therapeutic purposes [17]. The SELEX process is composed of isolating DNA or RNA sequences with high affinity and specificity for molecular targets from a random sequence pool. In order to select high-affinity aptamers, the process typically requires 8–15 rounds of enrichment, polymerase chain reaction (PCR) amplification, and nucleic acid purification [18]. Capillary electrophoresis (CE)-SELEX is able to select high-affinity aptamers in 2–4 cycles of isolation resulting in the shortening of the process [19]. CE-SELEX is a rapid method of aptamer isolation using CE. In this method, the nucleic acid sequences that bind to the target are separated from the non-binding sequences based on the differential velocity of migration [20]. A growing body of research has indicated that aptamers have the potential to be used as therapeutic agents in a wide variety of human disease types, including cancer, inflammatory, and CVD [21].

The development of aptamers against various molecular targets involved in CVDs has been an active field of aptamer research over the previous decade. Until now, the therapeutic applications of synthetic nucleic acid aptamers for CVDs include aptamers selected against thrombin, von Willebrand factor, factor IX, factor XII, P-selectin, and vascular endothelial growth factor (VEGF). Macugen (pegaptanib sodium) is the first Food and Drug Administration approved aptamer-based drug against VEGF, which is used for the treatment of neovascular age-associated macular degeneracy [22–24].

The advantages of aptamers compared with antibodies include a smaller size, lower immunogenicity in the body, lower toxicity and modification flexibility, and easy, rapid, and reliable synthesis. In addition, aptamers are useful compounds since the method used for their detection is fast, cheap, and credible with no complexity [25]. Accordingly, the present study aimed to design and synthesize aptamers in order to replace the antibodies used for PCSK9 inhibition. In the present study, ssDNA aptamers directed against PCSK9 were designed and selected using CE-SELEX followed by the characterization of their potency.

## Materials and Methods

### Chemicals

Recombinant human PCSK9 was purchased from Thermo Fisher Scientific, Inc. (Waltham, MA, USA). The purity and integrity of PCSK9 were initially confirmed using SDS-PAGE. The ssDNA library pool used for aptamer selection consisted of 52 random bases flanked by two primer regions, as follows: 5′-ATACCAGCTTATTCAATT-[52 random bases]-AGATTGCACTTACTATCT-3′. The aptamer library pool (ssDNA) and primers were all synthesized by Macrogen, Inc. (Seoul, Republic of Korea). Taq DNA Polymerase Master Mix was obtained from Ampliqon (Odense, Denmark). Lambda exonuclease III, used for the digestion of PCR products, and a GeneRuler 50 base pair DNA Ladder were purchased from Thermo Fisher Scientific, Inc. The molecular biology grade agarose powder, gel loading dye, and ethidium bromide for ssDNA characterization were purchased from Sigma-Aldrich (Merck KGaA, Darmstadt,

Germany). All the samples and buffers were prepared using a syringe filter unit of 0.22 μm (Merck KGaA).

## CE Selection of Aptamers

During the first step of CE-SELEX selection, the ssDNA library (including $10^{12}$–$10^{16}$ sequences) was heated to 90 °C for 5 min in tris (hydroxyamino) methane-glycine-potassium (TGK) buffer (25 mM Tris-HCl, 192 mM glycine, 5 mM KH2PO4, and pH 8.3) followed by a cooling down step on ice to allow for the formation of secondary structures. A total of 10 μM ssDNA library was used in the first selection round, and 5 μM purified ssDNA was used for the subsequent rounds. The target PCSK9 was then added to the ssDNA library to form a final concentration of 100 nM for the three rounds of CE selection. The ssDNA library was incubated with the PCSK9 at room temperature for at least 30 min to ensure that the binding reached equilibrium. CE-SELEX selection was performed using a 64.5-cm-long (with 56 cm to the detector) fused silica capillary (50-μm-inner diameter and 360-μm-outer diameter bare (uncoated)) on a 7100 capillary electrophorese system equipped with a photodiode array detector (Agilent Technologies, Inc., Santa Clara, CA, USA). The capillary was first washed with 0.1 M NaOH, deionized water, and TGK buffer, each for 5 min, prior to the injection of the incubation mixture at 50 mbar for 5 s. The mixture was separated under 15 kV voltage in TGK buffer at 25 °C and the separation was monitored using an ultraviolet (UV) absorbance detector at 260 nm. The PCSK9-aptamer complex migrated off the capillary prior to the unbound ssDNA and was collected into a vial containing 100-μL separation buffer (TGK, pH 7.4) at the capillary outlet. Subsequent to collecting the bound aptamer sequences, the voltage was turned off and the capillary was rinsed with TGK buffer for 5 min at high pressure to remove all unbound aptamer sequences.

In this study, the following equation was used to determine when the edge of the collection window achieves the capillary output: $t_{out} = \frac{(L_T)(t_{det})}{L_D}$, where tout is the time that the end of the collection window reaches the outlet, $L_T$ is the total length of the capillary, $L_D$ is the length from inlet to the detector, and $t_{det}$ is instead when the start of the collection window reaches the outlet.

## PCR Amplification and ssDNA Aptamer Generation

The collected sequences of the CE-SELEX aptamers were amplified using PCR to produce a novel oligonucleotide pool for the second round of selection. Initially, the optimum number of PCR cycles for the enrichment of the oligonucleotide pool with no specific amplicons were calculated. The preparative PCR reactions consisting of 8, 10, 12, and 15 cycles were then performed to obtain the 12 cycles of PCR that were selected and amplified to generate further PCR products for the preparation of the ssDNA aptamers required for the second round of selection. However, the third round consisted of 25 cycles of PCR for selection and amplification.

The PCR reaction mixture volume in each tube was 30 μL that contained 15 μL Taq DNA Polymerase Master Mix, 1-μL forward primer (5′-ATACCAGCTTATTCAATT-3′), 1-μL phosphate reverse primer (5′-p-AGATTGCACTTACTATCT-3′), 5-μL collected CE fraction, and 8-μL nuclease-free water. For each round, the PCR reaction and control (without collected DNA) tubes were placed in a thermal cycler and heated at 94 °C for 5 min to denature the DNA template and primers, followed by cycles of denaturation (94 °C for 30 s), annealing (53 °C for 30 s) and extension (72 °C for 30 s), and a final extension for 5 min at 72 °C. The success of amplification of the DNA template was confirmed by gel electrophoresis using a 2.5% agarose gel stained with ethidium bromide and visualization using a gel documentation system.

Following PCR amplification, the PCR products were digested with lambda exonuclease III and were then purified using Amicon centrifugal filters to obtain extra-pure ssDNAs for the next round of selection. Briefly, the PCR products were first incubated with lambda exonuclease III for 30 min at 37 °C. The enzyme was then inactivated by incubating the mixture at 80 °C for 15 min followed by purification of the desired forward DNA strand using Amicon® Ultra − 0.5 centrifugal filter (Merck KGaA) for the next round of selection. Eventually, a reverse transcription PCR technique was used for the identification of ssDNAs from the PCR products as previously described [26].

## DNA Cloning and Sequencing

Following three rounds of selection using CE-SELEX, the ssDNA sequences were amplified using PCR. The PCR products were initially purified using a MinElute PCR Purification kit (Qiagen GmbH, Hilden, Germany) based on the manufacturer's protocol and were then ligated using a TA cloning vector (Thermo Fisher Scientific, Inc.) using T4 DNA ligase. The recombinant TA vectors were then used to transform competent *E. coli* TOP10 cells (Pasteur Institute of Iran, Tehran, Iran). The transformed cells ($10^5$) were plated on Luria broth (LB) agar containing 100 μg/mL ampicillin. The positive clones (ampicillin resistance) were evaluated by colony PCR. The reaction mixture contained 12.5 μL Taq DNA Polymerase Master Mix, 2 μL each of forward (5′-TTGT AAAACGACGGCCAGT-3′) and reverse (5′-ACAG GAAACAGCTATGACCA-3′) M13 primers, 10.5-μL nuclease-free water, and the contaminated colony (as in the template), which was selected using a pipette tip that was then rinsed in the PCR tube. The total reaction volume was 25 μL. The PCR reaction consisted of one cycle at 96 °C for 180 s

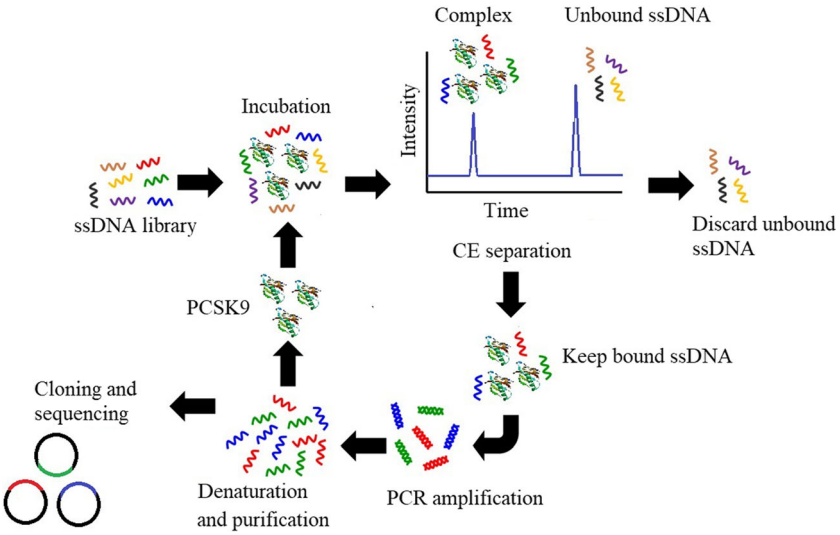


**Fig. 1** Schematic illustration of the steps in capillary electrophoresis evolution of ligands by exponential enrichment selection. ssDNA, single-stranded DNA; PCR, polymerase chain reaction; PCSK9, proprotein convertase subtilisin/kexin type 9

followed by 30 cycles at 96 °C for 30 s, 58 °C for 30 s, 72 °C for 30 s, and a cycle at 72 °C for 300 s in a thermal cycler.

Single colonies were randomly cultured in LB broth subsequent to growing the cells overnight on a LB agar plate at 37 °C, and additionally, the evaluation of positive clones was performed using colony PCR. The plasmids positively subcloned with the selected fragments were extracted from the cells cultured overnight in LB broth in an incubator shaker at 37 °C using the PrimePrep Plasmid DNA Extraction kit (GeNet Bio, Daejeon, Korea) based on the manufacturer's protocol. Ultimately, the extracted plasmids were sequenced using M13 universal primers (Macrogen, Inc.).

## Estimation of Secondary Structure

The secondary structures of the aptamers were predicted using the Mfold web server for nucleic acid folding and hybridization prediction [27]. Based on the obtained results, two aptamers with the highest thermodynamic stability and lowest Gibbs free energy (Δ*G*: kcal/mol) were selected for further assessments.

## Half Maximal Inhibitory Concentration ($IC_{50}$) and Dissociation Constant ($K_d$) Measurements

At first, the two selected aptamers with the highest thermodynamic stability were evaluated using an enzyme-linked immunosorbent assay (ELISA) method by a PCSK9-biotinylated-LDLR binding assay kit (BPS Bioscience, Inc., San Diego, USA; cat no. #72002) according to the manufacturer's protocol. In brief, microtiter plate wells coated with LDLR extracellular domain were incubated (4 °C, overnight) with biotinylated PCSK9 in the presence of serial dilutions (100, 200, 300, 400, and 500 nM) of the selected ssDNA aptamers. Following the washing step, the wells were incubated (1 h at 25 °C) with horseradish peroxidase (HRP)-labeled streptavidin and binding of PCSK9 to the LDLR extracellular domain was assessed by the addition of the HRP substrate and evaluation of the signals using a chemiluminescence microplate reader. The $IC_{50}$ and $K_d$ were measured by

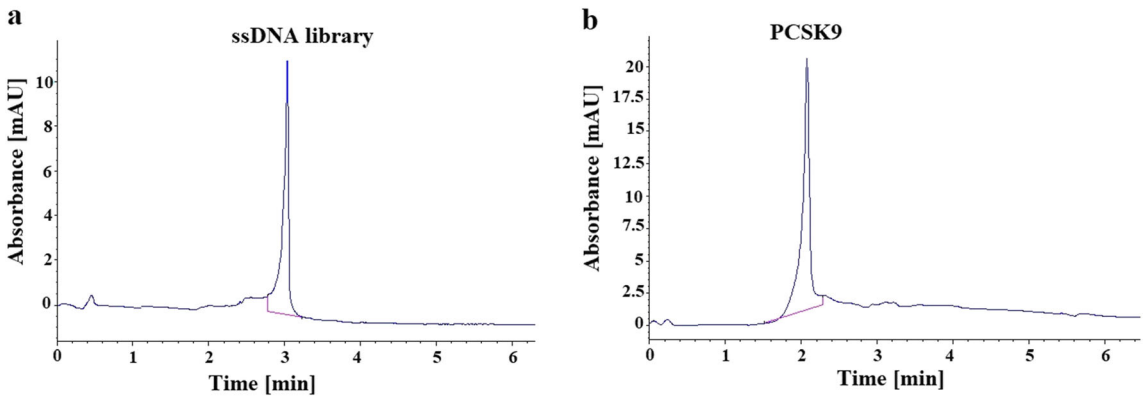


**Fig. 2** Capillary electrophorese electropherogram results. **a** Peak of the ssDNA library with a retention time of 3.065 min at 260 nm. **b** Peak of recombinant PCSK9 with a migration time of 2.076 min at 280 nm. Conditions for each experiment were exactly the same. mAU, milliabsorbant unit; ssDNA, single-stranded DNA; PCSK9, proprotein convertase subtilisin/kexin type 9

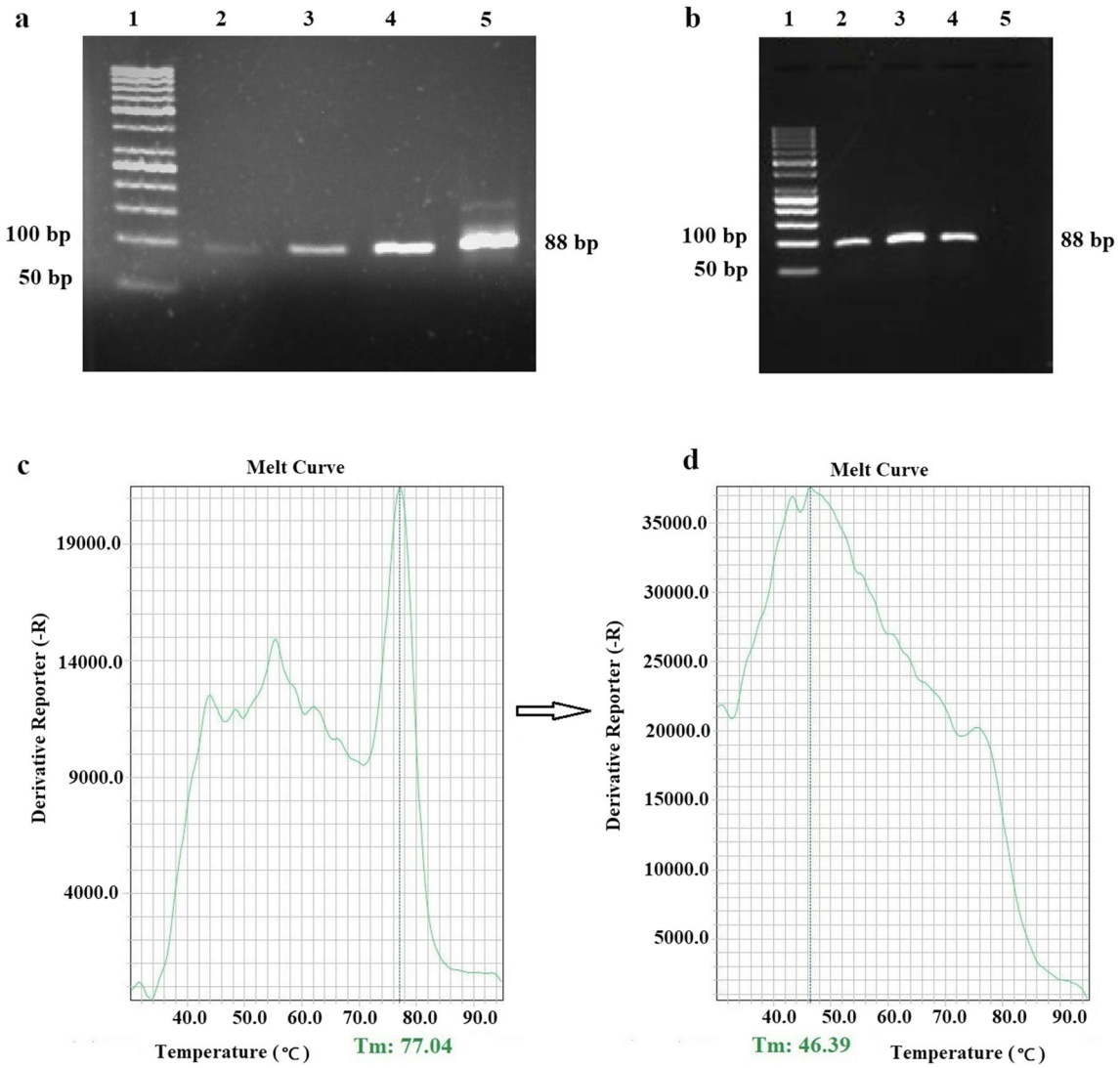


**Fig. 3** Agarose gel electrophoresis images. **a** Products of the different cycles of enriched DNA library amplification (lane 1, 50 bp ladder; lane 2, 8 cycles; lane 3, 10 cycles; lane 4, 12 cycles, and lane 5, 15 cycles). **b** Preparation of PCR for the second round of selection (lane 1, 50 bp ladder; lanes 2, 3, and 4, 12 cycles; and lane 5, negative control). Identification of PCR products and ssDNA using reverse transcriptase-PCR and melting curve analysis indicated that **c** double-stranded DNA converted to **d** ssDNA based on the substantial reduction of the Tm from 77.04 to 46.39 °C. ssDNA, single-stranded DNA; Tm, melting temperature; bp, base pair

monitoring the decrease in the intensity of the luminescence subsequent to binding to the aptamers, as previously described [28, 29].

## Statistical Analysis

A two-tailed Pearson's correlation analysis and one-way ANOVA followed by a post hoc Tukey test were used to analyze the data using GraphPad Prism 6 software (GraphPad Software, Inc., La Jolla, CA, USA). The data are presented as mean ± SEM. $P < 0.05$ was considered to indicate a statistically significant difference. Furthermore, the $IC_{50}$ value of the aptamer PCSK9 was evaluated using the following equation: Log (Cinhibitor) compared with response - variable slope. Furthermore, the $K_d$ was calculated using the equation of one site-specific binding using Hill slope as mentioned above the GraphPad Prism 6 software.

# Results

## CE-SELEX Selection

The schematic design of the CE-SELEX method is presented in Fig. 1. Briefly, a random ssDNA library, including 1012–1016 sequences, was incubated at a low concentration of PCSK9 and then separated using CE. The specific bound ssDNA sequences were separated from the unbound and non-specific ssDNAs. The ultra-pure and specific bound sequences were collected for amplification using PCR.

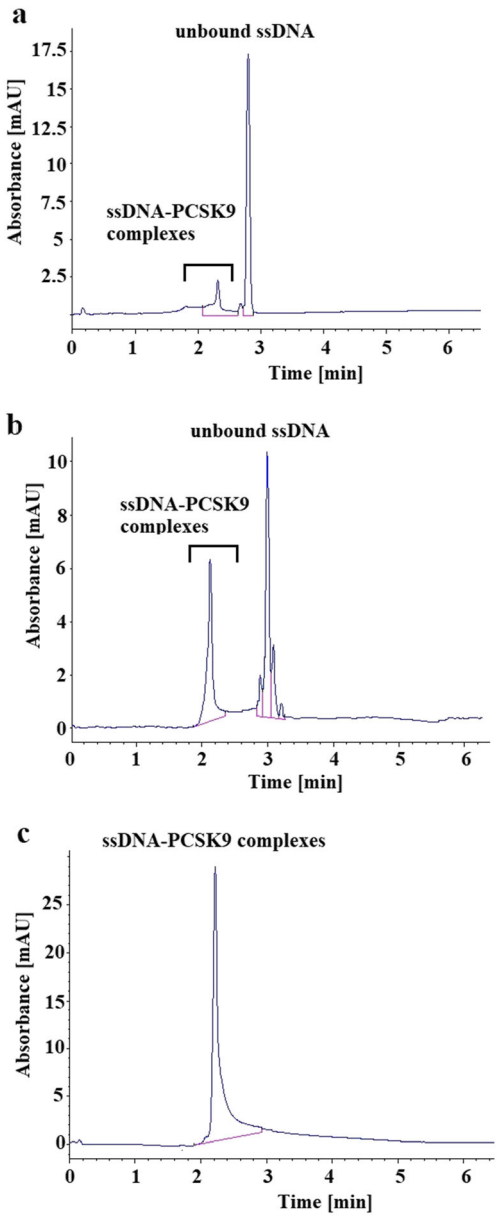


**Fig. 4** Selection of ssDNA aptamer selection using capillary electrophoresis evolution of ligands by exponential enrichment. **a** Electropherogram of the first round of ssDNA aptamer selection using UV detection (260 nm). **b** Electropherogram of the second round of ssDNA aptamer selection using UV detection (260 nm). **c** Electropherogram of the third round of ssDNA aptamer selection using UV detection (260 nm). ssDNA, single-stranded DNA; UV, ultraviolet; PCSK9, proprotein convertase subtilisin/kexin type 9; mAU, milli-absorbant unit

Consequently, the fraction of the bound sequences was enriched and purified followed by further amplification of the ssDNAs for the second round of CE selection. This process was repeated in order to achieve maximum affinity. Eventually, the high affinity and enriched ssDNAs were characterized by sequencing.

CE separates the components of an injected sample based on electrophoretic mobility and electroosmotic flow (EOF). Since the EOF is greater compared with the electrophoretic mobility of the sample components, all injected molecules migrate from the inlet (anode) to the outlet (cathode) of the capillary [30]. Considering that the negative charge of ssDNA sequences is higher compared with that of PCSK9 molecules, the unbound ssDNAs migrate slower compared with the ssDNA-PCSK9 complexes. Thus, the ssDNA-PCSK9 complexes were collected from the outlet of the capillary within the so-called collection window, which is the time between the beginning of the separation and the time at which unbound sequences reach the outlet.

In the present study, the specific aptamers with a high affinity against the PCSK9 protein were obtained using three rounds of CE-SELEX selection. To measure the separation time and the purity of the compounds, the ssDNA library (5 μM) and recombinant PCSK9 (1 μM) were individually injected into the fused silica capillary of the electrophorese system. The peaks were analyzed by a UV photodiode array detector at 260- and 280-nm wavelengths, simultaneously (Fig. 2).

The first round of separation was performed by incubating 10 μM ssDNA library with 100 nM PCSK9 for 30 min at room temperature. The success of this process was then assessed by UV absorbance detection (260 nm). The optimum number of PCR cycles (12 cycles) was determined and ssDNA was generated from double-stranded DNA (dsDNA) using lambda exonuclease digestion. The second round of separation was conducted by incubating 5 μM ssDNA library with 100 nM PCSK9 for 30 min at room temperature followed by an assessment by UV absorbance detection (260 nm). Figure 3 demonstrates the optimum cycle number of the preparative PCR for the second round of selection. Successful digestion of dsDNA with Lambda exonuclease was confirmed using the reverse transcription PCR (Fig. 3). Finally, the third round of selection was performed using a similar strategy as the previous steps, except for the optimum number of PCR cycles (25 cycles).

Considering that the mole ratio of the ssDNA library/PCSK9 was high in each round of separation by CE, there should not be any individual PCSK9 molecules without an aptamer attachment. Therefore, in Fig. 4, the first peak is associated with the ssDNA-PCSK9 complex, and the next peak is associated with the unbound ssDNA sequences. In the last cycle, all ssDNAs were bonded to the PCSK9 protein and no further separation was observed.

As presented in Fig. 4, the ssDNA-PCSK9 complexe peak gradually rose at each step of CE-SELEX. As the electropherograms of rounds 3 and 4 were similar, no further selection was performed.

To recognize the specificity of the ssDNA aptamers, 40 selected clones were analyzed. The plasmids were extracted from selected clones with an enriched ssDNA pool and then sequenced. In the present experiment, clones with aptamer

**Table 1** Determination and characterization of the selected aptamers

| Aptamer (clones) | ΔG (kcal/mol) | Sequences |
|---|---|---|
| AP-1 (clone 5) | − 9.17 | ATACCAGCTTATTCAATTGACCCGTTTCGTTCCCTCTGGGAAGT TTAGCCCAGTTGCCTGGGCGATACCAAGATAGTAAGTGCAATCT |
| AP-2 (clone 1) | − 8.28 | ATACCAGCTTATTCAATTTCTTCGCCAGTGCCAGGATCTCAGTT GGCGGTTCATTAGCTGGGTTGGTCGAAGATAGTAAGTGCAATCT |
| AP-3 (clone 6) | − 8.09 | ATACCAGCTTATTCAATTTTCAAAGTCAAGGGTTGCCTTGGTTC GCCCTGCGATAATACGCGGTTCCCTCAGATAGTAAGTGCAATCT |
| AP-4 (clone 27) | − 6.20 | ATACCAGCTTATTCAATTGGCATGGTAATTTCACAGCTGCCTCT TCGATGCTCCAACTGGAGTAGGGCCGAGATAGTAAGTGCAATCT |
| AP-5 (clone 38) | − 6.32 | ATACCAGCTTATTCAATTTGTAATGGTCCCGCAGGTTCCCCCTT TCCTACGGCATGACAGGTCGCTGCGCAGATAGTAAGTGCAATCT |
| AP-6 (clone 8) | − 6.51 | ATACCAGCTTATTCAATTTCGATGGGTCGGTTTCCCCGCAAAGT GGCCCTCGCTTATACCCAACAGCGCCAGATAGTAAGTGCAATCT |
| AP-7 (clone 13) | − 5.79 | ATACCAGCTTATTCAATTATTCGTGTACGGATCATTGTGCCCCG GCTACGTTTGGAGCGGTTGTGCATGAAGATAGTAAGTGCAATCT |
| AP-8 (clone 21) | − 5.03 | ATACCAGCTTATTCAATTTTAATCGTCGACATCACACGGGCCTT TAACTTTTTTAAAAGGTGATCTGGTCAGATAGTAAGTGCAATCT |
| AP-9 (clone 34) | − 3.53 | ATACCAGCTTATTCAATTTGATGGTCATCGGTCAAATCATCCTG AGGTCTGTTGTGTAATGATTCTGTGAAGATAGTAAGTGCAATCT |
| AP-10 (clone 19) | − 3.78 | ATACCAGCTTATTCAATTCTATTTTTCTACCTAGAGTATGCAAT TCGAAAGGCTATCCCTGTAGGTTGTGAGATAGTAAGTGCAATCT |

sequences containing 88 base pairs were selected. The results indicated the presence of 10 different aptamers with similar conserved regions (Table 1).

### $IC_{50}$ and $K_d$ of the Selected Aptamers

The secondary structure of the selected ssDNA aptamers was predicted using the Mfold web server. The calculations indicated that two of the aptamers, namely aptamer 1 (AP-1) and aptamer 2 (AP-2), were preferred compared with the other 8 due to possessing the highest structural thermodynamic stability with $\Delta G$ of − 13.06, − 9.17 kcal/mol and − 12.94, − 8.28 kcal/mol at 25 °C and 37 °C, respectively (Fig. 5a and b). Based on the obtained results, two aptamers with the highest thermodynamic stability and lowest Gibbs free energy ($\Delta G$: kcal/mol) were selected for further assessments.

Consequently, the selected aptamers, which presented the highest thermodynamic stability, were synthesized and evaluated by an ELISA method using a PCSK9-biotinylated-LDLR binding assay which has a high sensitivity for the detection of biotin-labeled PCSK9 by streptavidin HRP. Serial dilutions of AP-1 and AP-2 aptamers (100, 200, 300, 400, and 500 nM) were prepared and assessed using a chemiluminescence reader.

The $IC_{50}$ and $K_d$ values were calculated for the two thermodynamically selected aptamers by monitoring the decrease in luminescence intensity subsequent to binding to the aptamers. Thus, the increase in the aptamer concentrations in addition to the inhibition of PCSK9 resulted in a decreased luminescence intensity. The $IC_{50}$ and $K_d$ values were calculated using GraphPad Prism 6 software. AP-1 presented the highest binding affinity for PCSK9 with a $K_d$ value of 294 nM and a very low $IC_{50}$ value of 325 nM (Fig. 6a and b). Furthermore, the $K_d$ and $IC_{50}$ values for AP-2 were 323 nM and 327 nM, respectively (Fig. 6c and d).

Inhibition of PCSK9-biotinylated-LDLR by aptamers. In addition to the screening and profiling experiments, the inhibition of PCSK9-biotinylated-LDLR by the selected aptamers was also evaluated. As presented in Fig. 7, the test inhibitors AP-1 and AP-2 together with the negative and positive controls were evaluated by increasing the concentration of AP-1 and AP-2. The intensity of the luminescence of the tests was analyzed. The luminescence intensity ($P < 0.05$) was significantly decreased, compared with the positive control, in the presence of test inhibitors AP-1 and AP-2, while no significant changes were detected in the positive or negative controls.

## Discussion

Statistically, CVD is one of the leading causes of mortality globally [31]. FH, as a type IIa hyperlipidemia, serves an important function in premature CVD [32]. In fact, serum LDL-C elevation is one of the major risk factors for coronary artery diseases, by increasing the formation of atherosclerotic plaques. PCSK9 was identified in 2003 when gain-of-function mutations in this gene were introduced as a third gene associated with FH and the cause of autosomal dominant

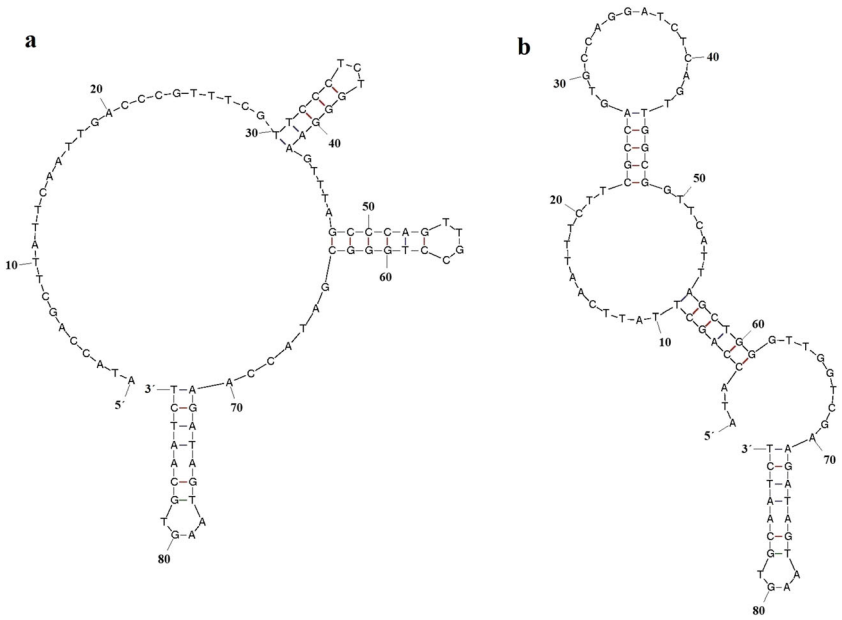


**Fig. 5** Secondary structure of AP-1 and AP-2. Secondary structure of **a** AP-1 with $\Delta G = -9.17$ kcal/mol and **b** AP-2 with $\Delta G = -8.28$ kcal/mol. AP-1, aptamer 1; AP-2, aptamer 2

hypercholesterolemia [33]. PCSK9 serves a crucial role in the metabolism of LDL-C through interaction with LDLR followed by its destruction, which results in reduced LDLR levels on the plasma membrane in addition to elevated LDL-C plasma levels [34]. The function of PCSK9, as one of the emerging pathways that regulate cholesterol metabolism, has resulted in researchers initiating efforts to examine PCSK9 as a potential target for LDL-C reduction.

The main aim of developing PCSK9 inhibitors as a form of therapy is to reduce serum LDL-C levels by limiting PCSK9 activity. Inhibition of PCSK9 activity results in a decrease in the LDLR degradation rate, followed by an increase in the

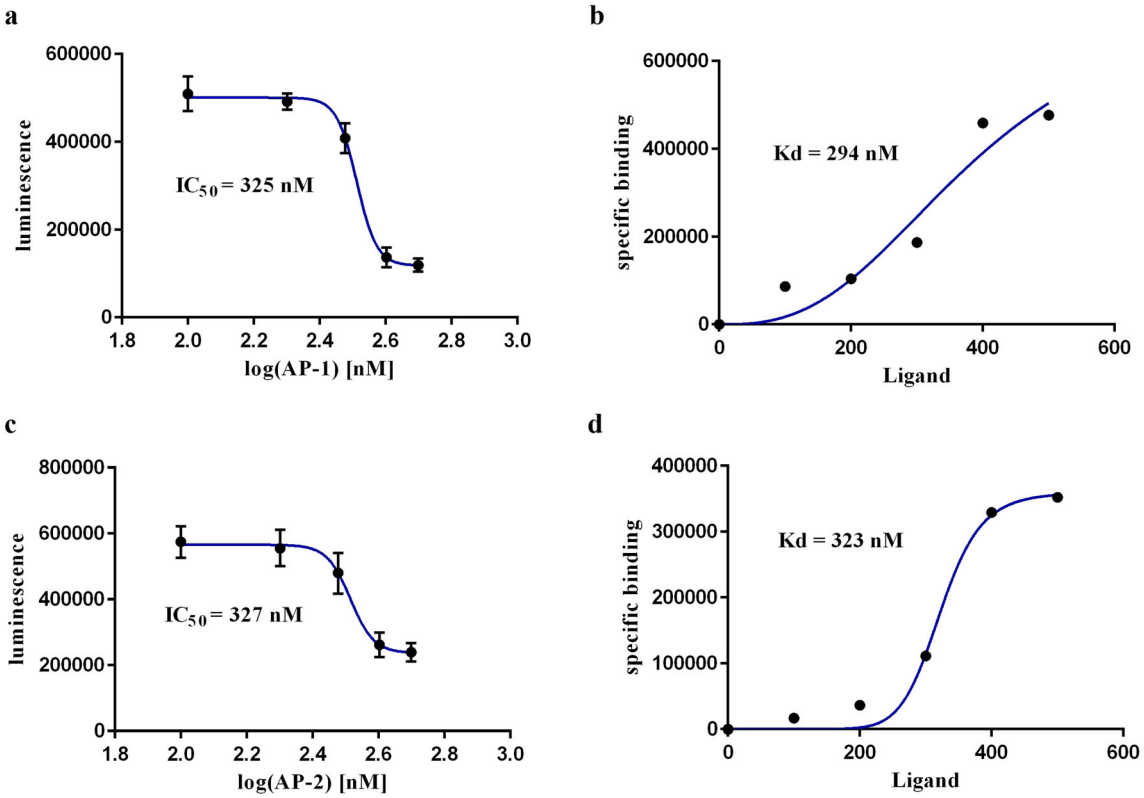


**Fig. 6** $IC_{50}$ and $K_d$ of AP-1 and AP-2. Calculation of the **a** $IC_{50}$ and **b** Kd of AP-1 and the **c** $IC_{50}$ and **d** $K_d$ of AP-2 with GraphPad Prism 6 software. $IC_{50}$, half maximal inhibitory concentration; $K_d$, lowest dissociation constant; AP-1, aptamer 1; AP-2, aptamer 2

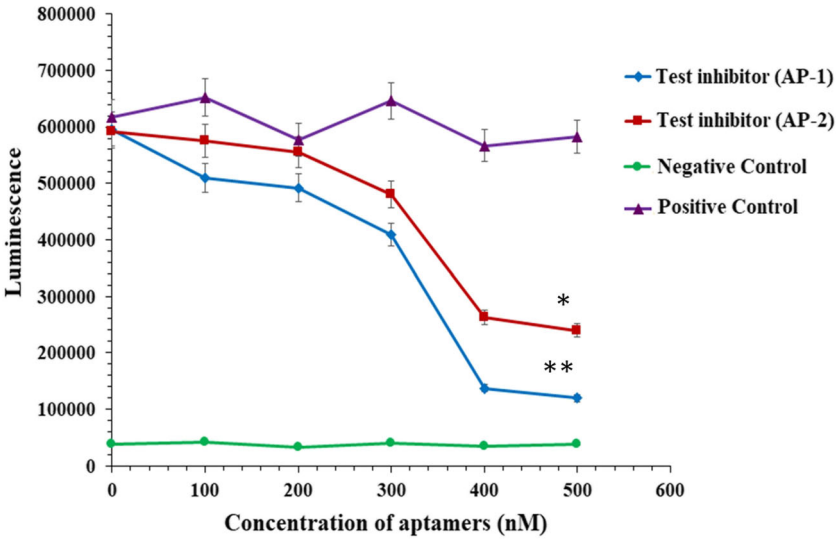


**Fig. 7** Luminescence intensity with aptamer concentrations compared with positive and negative controls. The positive and negative controls were groups treated with and without proportion convertase subtilisin/kexin type 9 inhibitor, respectively. $P < 0.05$. AP-1, aptamer 1; AP-2, aptamer 2. The asterisks on the graph indicate there are significant differences between AP-1 (**) and AP-2 (*) compared with positive control

expression level of LDLR on the surface of hepatocytes, which consequently results in a decrease in the plasma level of LDL-C [35]. The results of landmark clinical trials have indicated that drugs targeting PCSK9 potently reduce LDL-C levels [14]. One study has demonstrated that treatment with PCSK9 inhibitors considerably lowers the risk of CVD [36].

Some of the numerous advantages of aptamers compared with antibodies include their small size, extensive clinical applicability, non-immunogenic and non-toxic properties, and, more importantly, the low cost of production and high biological stability [37]. Recently, synthetic oligonucleotide aptamers against a cluster of differentiation 20 have been introduced [38]. Aptamer-conjugated liposome for gene or drug delivery system which delivered loaded ligands to target cells with certain specificity and efficiency could be a useful tool for therapeutic purposes [39].

Designing and selecting aptamers that prevent the binding of PCSK9 to LDLR may increase the number of LDLR on the membrane of hepatocytes and subsequently decrease the plasma levels of LDL-C.

The separation of the protein-aptamer complex using CE is undertaken based on charge, ion size, hydrophobicity, and stereo-specificity. The separated aptamers are highly selective with stereo-specificity and with no tendency to form non-specific binding interactions with non-specific proteins. Therefore, the CE-SELEX method is a powerful technique for the selection and separation of aptamers from a pool of DNA aptamers ($> 10^{12}$) for the specific inhibition of PCSK9 activity. Each round of CE-SELEX is sensitive and accurate. Following 3 rounds of CE selection, a few aptamers (3 to 10) that finally bound to PCSK9 were separated and amplified using PCR. The selected aptamer pool was definitely heterogeneous; therefore, cloning and sequencing were performed in order to transform the pool into a single distinct sequence. Consequently, a single aptamer was selected for further evaluation, including the determination of its three-dimensional structure, thermodynamic stability, inhibitory concentration, affinity potency, and finally calculating $IC_{50}$ and $K_d$ values. Considering the obtained results in addition to the highest affinity and selectivity, two aptamers, namely AP-1 and AP-2, which presented the highest thermodynamic stability, were selected and synthesized for further experiments. The Gibbs free energy of AP-1and AP-2 at 25 °C and 37 °C is lower than the other 8 aptamers. Therefore, both aptamers are stable at 25 °C and 37 °C.

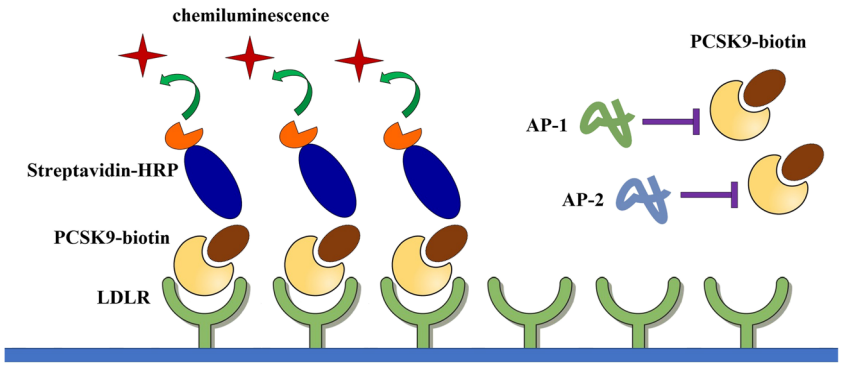


**Fig. 8** Schematic representation of the mechanism of PCSK9 inhibition by AP-1 and AP-2. PCSK9, proprotein convertase subtilisin/kexin type 9; AP-1, aptamer 1; AP-2, aptamer 2; HRP, horseradish peroxidase; LDLR, low-density lipoprotein receptor

The calculated $IC_{50}$ values of AP-1 and AP-2 were 325 and 327 nM, respectively. These $IC_{50}$ values indicate the potency of AP-1 and AP-2 to inhibit the biochemical function of PCSK9. In general, if the agonist activity reaches the lowest level of its biological function when there is the lowest level of inhibitor concentration available, that is a suitable concentration for treatment. Therefore, the lowest concentration of AP-1 and AP-2 in inhibiting the PCSK9 was considered to be an acceptable level. The affinity of AP-1 and AP-2 to bind to PCSK9 reflects the $K_d$, that is, a measure of the propensity of the PCSK9-aptamer complex to dissociate reversibly. $K_d$ is a thermodynamic parameter and is temperature dependent. AP-1 and AP-2 have a reliable $K_d$ at 37 °C that represents the physiological condition.

Although the validation of the affinity and specificity using conventional methods, including CE and surface plasmon resonance (SPR), was a limitation of the present study for prediction of $K_d$, the CE approach was used for aptamer selection in order to achieve the optimal inhibitory effects of the ssDNA library. It is clear that the aptamers collected from the CE outlet presented the highest affinity and specificity for PCSK9 following three rounds of separation in CE. Therefore, the aptamers, which were selected in difficult conditions of CE, were targeted in the present study. The intended aptamers should present the lowest $K_d$; however, it was not possible to measure the exact $K_d$ value when using CE. Nevertheless, measuring the exact amount of $K_d$ was not necessary and the temperature was not a key factor at this stage of the study. In the present study, the potency of the selected aptamers to inhibit PCSK9 was reflected by their $IC_{50}$ and $K_d$ measured using a kit. Therefore, a relative $K_d$ value was reported in the present study. The purpose of the present study was to identify an aptamer with a stable conformation (lowest $\Delta G$) and a high potency for the inhibition of PCSK9. Although the binding of PCSK9 to LDLR is pH dependent, the aim of the present study was to identify the optimal aptamer in terms of inhibitory function to prevent PCSK9 from binding to LDLR at normal pH levels.

PCSK9 is mainly synthesized in the liver and is known to function as a negative regulator of hepatic LDLRs by binding to the LDLR ectodomain. PCSK9 regulates plasma LDL-C levels by diverting the cell-surface LDLR of hepatocytes to lysosomes for degradation. Thus, PCSK9 plasma levels directly influence the level of circulating LDL-C. Therefore, any compound that inhibits or neutralizes PCSK9 directly or indirectly triggers the lowering serum LDL-C [40]. In order to characterize the inhibitor specificity of AP-1 and AP-2 against PCSK9, an ELISA binding assay was performed. The assay was designed for PCSK9 screening and profiling purposes [28, 29]. The two novel aptamers identified, AP-1 and AP-2, presented excellent inhibitory effects against PCSK9, which interfere with the PCSK9-LDLR interaction (Fig. 8).

Finally, AP-1 and AP-2 were designed, selected, characterized, and introduced as appropriate inhibitors of PCSK9. Furthermore, the potency and efficacy of the antibodies and aptamers to inhibit PCSK9 were not compared in the present study. Further experiments are also required to evaluate the specificity, toxicity, pharmacokinetics, and other associated aspects of these aptamers in cell culture and animal models.

**Acknowledgments** The authors acknowledge the Isfahan University of Medical Sciences for providing academic and laboratory supports.

**Author's Contributions** AAP conceived the study, designed the experiments, performed the capillary electrophoresis evolution of ligands by exponential enrichment, and analyzed the data. RS prepared the samples for capillary electrophoresis and performed the experiments. HK facilitated the molecular biology experiments.

**Funding Information** The present study was supported by the Iran National Science Foundation (INSF grant no. 93016087) and the Isfahan University of Medical Sciences (project no. 395902).

**Data Availability** The datasets used and/or analyzed during the current study are included in this published article.

## Compliance with Ethical Standards

**Conflict of Interest** The authors declare that they have no conflict interests.

**Ethics Approval and Consent to Participate** This study was approved by the Ethics Committee (no. 395902) of the Isfahan University of Medical Sciences, Iran.

**Patient consent for publication** Not applicable.

## References

1. Levine GN, Lange RA, Bairey-Merz CN, Davidson RJ, Jamerson K, Mehta PK, et al. Meditation and cardiovascular risk reduction: a scientific statement from the American Heart Association. J Am Heart Assoc. 2017;6(10):e002218.
2. Sniderman AD, Islam S, Yusuf S, McQueen MJ. Discordance analysis of apolipoprotein B and non-high density lipoprotein cholesterol as markers of cardiovascular risk in the INTERHEART study. Atherosclerosis. 2012;225(2):444–9.
3. Defesche JC, Gidding SS, Harada-Shiba M, Hegele RA, Santos RD, Wierzbicki AS. Familial hypercholesterolaemia. Nat Rev Dis Primers. 2017;3:17093.
4. Wilson PW, D'Agostino RB, Levy D, Belanger AM, Silbershatz H, Kannel WB. Prediction of coronary heart disease using risk factor categories. Circulation. 1998;97(18):1837–47.
5. Nicholls SJ, Ballantyne CM, Barter PJ, Chapman MJ, Erbel RM, Libby P, et al. Effect of two intensive statin regimens on progression of coronary disease. N Engl J Med. 2011;365(22):2078–87.
6. Hovingh GK, Davidson MH, Kastelein JJ, O'connor AM. Diagnosis and treatment of familial hypercholesterolaemia. Eur Heart J. 2013;34(13):962–71.
7. Seidah NG, Benjannet S, Wickham L, Marcinkiewicz J, Jasmin SB, Stifani S, et al. The secretory proprotein convertase neural

apoptosis-regulated convertase 1 (NARC-1): liver regeneration and neuronal differentiation. Proc Natl Acad Sci U S A. 2003;100(3):928–33.
8. Abifadel M, Varret M, Rabès J-P, Allard D, Ouguerram K, Devillers M, et al. Mutations in PCSK9 cause autosomal dominant hypercholesterolemia. Nat Genet. 2003;34(2):154–6.
9. Burke AC, Dron JS, Hegele RA, Huff MW. PCSK9: regulation and target for drug development for dyslipidemia. Annu Rev Pharmacol Toxicol. 2017;57:223–44.
10. Seidah NG, Awan Z, Chrétien M, Mbikay M. PCSK9: a key modulator of cardiovascular health. Circ Res. 2014;114(6):1022–36.
11. Dahagam C, Goud A, Abdelqader A, Hendrani A, Feinstein MJ, Qamar A, et al. PCSK9 inhibitors and their role in high-risk patients in reducing LDL cholesterol levels: evolocumab. Future Cardiol. 2016;12(2):139–48.
12. Wang X, Raghavan A, Chen T, Qiao L, Zhang Y, Ding Q, et al. CRISPR-Cas9 targeting of PCSK9 in human hepatocytes in vivo. Arterioscler Thromb Vasc Biol. 2016;36(5):783–6.
13. Gustafsen C, Kjolby M, Nyegaard M, Mattheisen M, Lundhede J, Buttenschøn H, et al. The hypercholesterolemia-risk gene SORT1 facilitates PCSK9 secretion. Cell Metab. 2014;19(2):310–8.
14. Dadu RT, Ballantyne CM. Lipid lowering with PCSK9 inhibitors. Nat Rev Cardiol. 2014;11(10):563–75.
15. He N-y, Li Q, Wu C-y, Ren Z, Gao Y, Pan L-h, et al. Lowering serum lipids via PCSK9-targeting drugs: current advances and future perspectives. Acta Pharmacol Sin. 2017;38(3):301.
16. Ellington AD, Szostak JW. In vitro selection of RNA molecules that bind specific ligands. Nature. 1990;346(6287):818–22.
17. Zhou J, Rossi J. Aptamers as targeted therapeutics: current potential and challenges. Nat Rev Drug Discov. 2017;16(3):181–202.
18. Liu J, You M, Pu Y, Liu H, Ye M, Tan W. Recent developments in protein and cell-targeted aptamer selection and applications. Curr Med Chem. 2011;18(27):4117–25.
19. Mosing RK, Mendonsa SD, Bowser MT. Capillary electrophoresis-SELEX selection of aptamers with affinity for HIV-1 reverse transcriptase. Anal Chem. 2005;77(19):6107–12.
20. Dong L, Tan Q, Ye W, Liu D, Chen H, Hu H, et al. Screening and identifying a novel ssDNA aptamer against alpha-fetoprotein using CE-SELEX. Sci Rep. 2015;5:15552.
21. Wang P, Yang Y, Hong H, Zhang Y, Cai W, Fang D. Aptamers as therapeutics in cardiovascular diseases. Curr Med Chem. 2011;18(27):4169–74.
22. Kaur H, Bruno JG, Kumar A, Sharma TK. Aptamers in the therapeutics and diagnostics pipelines. Theranostics. 2018;8:4016–32.
23. Povsic TJ, Vavalle JP, Alexander JH, Aberle LH, Zelenkofske SL, Becker RC, et al. Use of the REG1 anticoagulation system in patients with acute coronary syndromes undergoing percutaneous coronary intervention: results from the phase II RADAR-PCI study. EuroIntervention. 2014;10(4):431–8.
24. Jilma-Stohlawetz P, Gorczyca ME, Jilma B, Siller-Matula J, Gilbert JC, Knöbl P. Inhibition of von Willebrand factor by ARC1779 in patients with acute thrombotic thrombocytopenic purpura. Thromb Haemost. 2011;105(03):545–52.
25. Hamedani NS, Müller J. Capillary electrophoresis for the selection of DNA aptamers recognizing activated protein C. Methods Mol Biol. 2016;1380:61–75.
26. Kouhpayeh S, Hejazi Z, Khanahmad H, Rezaei A. Real-time PCR: an appropriate approach to confirm ssDNA generation from PCR product in SELEX process. Iran J Biotechnol. 2017;15(2):143–8.
27. Zuker M. Mfold web server for nucleic acid folding and hybridization prediction. Nucleic Acids Res. 2003;31(13):3406–15.
28. Chan JC, Piper DE, Cao Q, Liu D, King C, Wang W, et al. A proprotein convertase subtilisin/kexin type 9 neutralizing antibody reduces serum cholesterol in mice and nonhuman primates. Proc Natl Acad Sci U SA. 2009;106(24):9820–5.
29. Liang H, Chaparro-Riggers J, Strop P, Geng T, Sutton JE, Tsai D, et al. Proprotein convertase substilisin/kexin type 9 antagonism reduces low-density lipoprotein cholesterol in statin-treated hypercholesterolemic nonhuman primates. J Pharmacol Exp Ther. 2012;340(2):228–36.
30. Heiger DN. High performance capillary electrophoresis: an introduction: a primer. Agilent Technologies; 2000.
31. Agarwal SK, Avery CL, Ballantyne CM, Catellier D, Nambi V, Saunders J, et al. Sources of variability in measurements of cardiac troponin T in a community-based sample: the atherosclerosis risk in communities study. Clin Chem. 2011;57(6):891–7.
32. Benjamin EJ, Blaha MJ, Chiuve SE, Cushman M, Das SR, et al. Heart disease and stroke statistics—2017 update: a report from the American Heart Association. Circulation. 2017;135(10):E146.
33. Cohen JC, Boerwinkle E, Mosley TH Jr, Hobbs HH. Sequence variations in PCSK9, low LDL, and protection against coronary heart disease. N Engl J Med. 2006;354(12):1264–72.
34. Abifadel M, Elbitar S, El Khoury P, Ghaleb Y, Chémaly M, Moussalli M-L, et al. Living the PCSK9 adventure: from the identification of a new gene in familial hypercholesterolemia towards a potential new class of anticholesterol drugs. Curr Atheroscler Rep. 2014;16(9):439.
35. Seidah NG. The PCSK9 revolution and the potential of PCSK9-based therapies to reduce LDL-cholesterol. Glob Cardiol Sci Pract. 2017;1:e201702.
36. Chaudhary R, Garg J, Shah N, Sumner A. PCSK9 inhibitors: a new era of lipid lowering therapy. World J Cardiol. 2017;9(2):76–91.
37. Dunn MR, Jimenez RM, Chaput JC. Analysis of aptamer discovery and technology. Nat Rev Chem. 2017;1(10):0076.
38. Haghighi M, Khanahmad H, Palizban A. Selection and characterization of single-stranded DNA aptamers binding human B-cell surface protein CD20 by cell-SELEX. Molecules. 2018;23(4):e715.
39. Palizban AA, Salehi R, Nori N, Galehdari H. In vivo transfection rat small intestine K-cell with pGIP/Ins plasmid by DOTAP liposome. J Drug Target. 2007;15(5):351–7.
40. Stoekenbroek RM, Lambert G, Cariou B, Hovingh GK. Inhibiting PCSK9 - biology beyond LDL control. Nat Rev Endocrinol. 2018;15(1):52–62.